# Polarity Effects on the Photophysics of Dendrimers with an Oligophenylenevinylene Core and Peripheral Fullerene Units

**Manuel Gutierrez-Nava,[a] Gianluca Accorsi,[b] Patrick Masson,[a] Nicola Armaroli,*[b] and Jean-François Nierengarten*[a, c]**

*Dedicated to Dr. Jean-Pierre Sauvage on the occasion of his 60th birthday*

**Abstract:** Highly soluble dendritic branches with fullerene subunits at the periphery and a carboxylic acid function at the focal point have been prepared by a convergent approach. They have been attached to an oligophenylenevinylene (OPV) core bearing two alcohol functions to yield dendrimers with two, four or eight peripheral $C_{60}$ groups. Their photophysical properties have been systematically investigated in solvents of increasing polarity; that is, toluene, dichloromethane, and benzonitrile. Ultrafast OPV→$C_{60}$ singlet energy transfer takes place for the whole series of dendrimers, whatever the solvent. Electron transfer from the fullerene singlet is thermodynamically allowed in $CH_2Cl_2$ and benzonitrile, but not in apolar toluene. For a given solvent, the extent of electron transfer, signaled by the quenching of the fullerene fluorescence, is not the same along the series, despite the fact that identical electron transfer partners are present. By increasing the dendrimer size, electron transfer is progressively more difficult due to isolation of the central OPV core by the dendritic branches, which hampers solvent induced stabilization of charge separated couples. Compact structures of the hydrophobic dendrimers are favored in solvents of higher polarity. These structural effects are also able to rationalize the unexpected trends in singlet oxygen sensitization yields.

**Keywords:** dendrimers · electron transfer · energy transfer · fullerenes · singlet oxygen

## Introduction

The unique electronic properties of $C_{60}$ have generated significant research activities focused on its use as an electron and/or energy acceptor in photoactive multicomponent systems.[1] Of particular interest is the combination of the carbon sphere with π-conjugated oligomers for the construction of donor–fullerene arrays. On one hand, such derivatives have been used as the active layer in organic photovoltaic cells.[2–4] This molecular approach appears to be particularly interesting since the behavior of a unique molecule in a solar cell and the study of its electronic properties means one can easily obtain structure/activity relationships leading to a better understanding of the photovoltaic conversion.[4] On the other hand, covalently linked fullerene–(π-conjugated oligomer) systems show excited state interactions making them excellent candidates for fundamental photophysical studies. Generally, the light energy absorbed by the π-conjugated system is promptly convoyed to the fullerene sphere by an ultrafast singlet–singlet energy transfer process.[2–6] For example, this particular behavior has been used for the design of dendritic systems with light-harvesting properties.[7] In these compounds, a fullerene core unit acting as terminal energy receptor has been functionalized with dendritic branches bearing an array of peripheral chromophores collecting the light energy. It can be added that the initial energy transfer event observed in fullerene–(π-conjugated oligomer) ensembles populates the lowest fullerene singlet excited state which is capable of promoting electron transfer from the oligomer to the $C_{60}$ unit.[2–7] Actually, this is only the case when the charge separated state is lower in energy

[a] Dr. M. Gutierrez-Nava, Dr. P. Masson, Dr. J.-F. Nierengarten
Institut de Physique et Chimie des Matériaux de Strasbourg
Université Louis Pasteur et CNRS (UMR 7504)
23 rue du Loess, 67037 Strasbourg (France)
E-mail: jfnierengarten@chimie.u-strasbg.fr

[b] Dr. G. Accorsi, Dr. N. Armaroli
Instituto Per la Sintesi Organica e la Fotoreattività
Laboratorio di Fotochimica, Consiglio Nazionale delle Ricerche CNR
Via Gobetti 101, 40129 Bologna (Italy)
Fax: (+39) 051-639-9844
E-mail: armaroli@isof.cnr.it

[c] Dr. J.-F. Nierengarten
New address:
Groupe de Chimie des Fullerènes et des Systèmes Conjugués
Ecole Européenne de Chimie, Polymères et Matériaux (ECPM)
Université Louis Pasteur et CNRS, 25 rue Becquerel
67087 Strasbourg Cedex 2 (France)
Fax: (+33) 390-24-27-06



DOI: 10.1002/chem.200400157

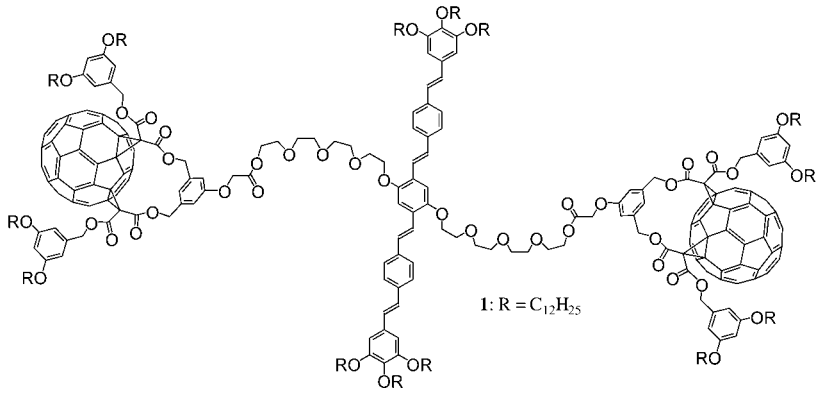


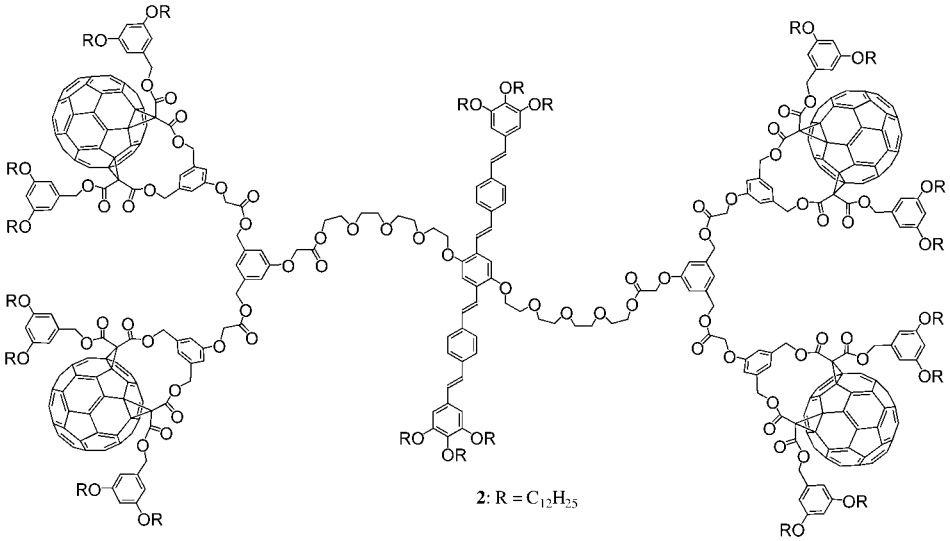


than the fullerene singlet. Thus, the cascade of photoinduced processes can be easily modulated by changing the donating ability of the conjugated system.[2c] Interestingly, when the energy level of the charge separated state is close to the fullerene singlet, the deactivation pathways are sensitive to the polarity of the solvent.[2–7] For example, Hummelen, Janssen and co-workers have reported the photophysical properties of an oligophenylenevinylene (OPV)–$C_{60}$ conjugate in solvents of different polarity.[3a] In apolar solvents such as toluene, the charge separated state is higher in energy than the first fullerene singlet and triplet excited states. Therefore, the light energy absorbed by the OPV fragment promptly conveyed to the fullerene lowest singlet excited state via energy transfer cannot yield charge separation anymore. In more polar solvents, the situation changes dramatically. Effectively, the energy of the charge-separated state drops below that of the first fullerene singlet excited state allowing occurrence of electron transfer after the initial energy transfer event. The latter two-step process was confirmed by kinetic studies revealing a close correspondence of the experimental results with the relative ordering of the various excited states as derived from theoretical calculations.[3a] Similar findings have been reported by Martin, Guldi and co-workers[7b] for a series of oligonaphthylenevinylene–fullerene dyads and by us for fullerene derivatives covalently linked to OPV simple fragments[2d] or dendritic wedges.[7a]

In this paper, we report the synthesis and the photophysical properties of dendrimers **1**–**3** with an OPV central core and $C_{60}$ terminal units. Whereas the first generation compound **1** shows the expected solvent dependent photophysical behavior, the last generation compound is almost not affected by changes in polarity as a result of dendritic encapsulation.

## Results and discussion

**Synthesis**: The synthesis of fullerodendrimers **1**–**3** was achieved by a convergent approach. To this end, dendritic branches with peripheral fullerene subunits were prepared first from **G1CO$_2$*t*Bu** (Scheme 1). This $C_s$ symmetrical fullerene bis-adduct was obtained in ten steps according to a previously reported procedure.[8] **G1CO$_2$*t*Bu** is actually easily prepared on a multi-gram scale and is highly soluble in common organic solvents owing to the presence of the four dodecyl chains. Therefore, it appears to be an excellent candidate for the preparation of fullerene-containing dendrons by using the synthetic strategy developed by some of us.[9] The latest is based on the successive cleavage of a *tert*-butyl ester moiety under acidic conditions followed by a *N*,*N*′-dicyclohexylcarbodiimide (DCC)-mediated esterification reaction. Thus, treatment of **G1CO$_2$*t*Bu** with $CF_3CO_2H$ in $CH_2Cl_2$ gave **G1CO$_2$H** in a quantitative yield and subsequent reaction with diol **4**[8] under esterification conditions using DCC, 1-hydroxybenzotriazole (HOBt) and 4-dimethylaminopyridine (DMAP) led to the *tert*-butyl protected dendron **G2CO$_2$*t*Bu** of second generation in 67% yield. The structure of **G2CO$_2$*t*Bu** was easily established based on its $^1$H and $^{13}$C NMR spectra. In addition, the MALDI-TOF mass spectrum showing the expected molecular ion peak also confirmed the structure of **G2CO$_2$*t*Bu**.

The $^1$H NMR spectrum of **G2CO$_2$*t*Bu** is shown in Figure 1 together with the spectrum of the corresponding first generation derivative **G1CO$_2$*t*Bu**. Both spectra show the characteristic features of $C_s$ symmetrical 1,3-phenylenebis(methy-

  

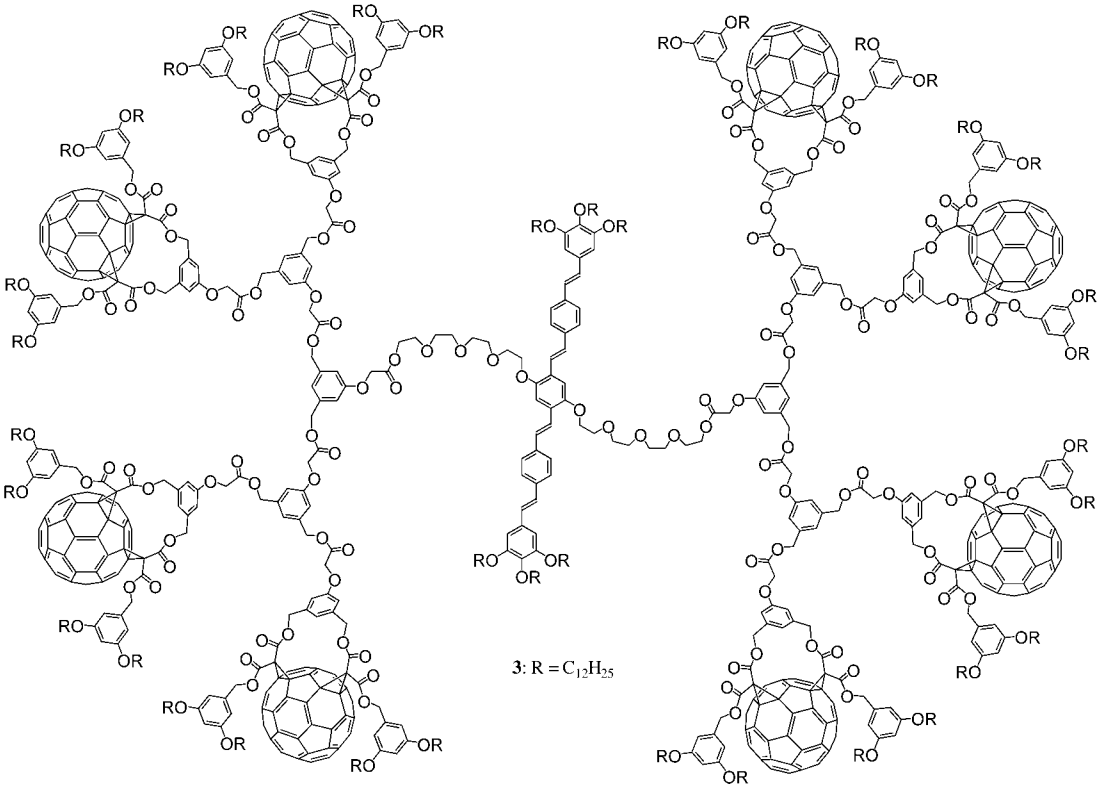


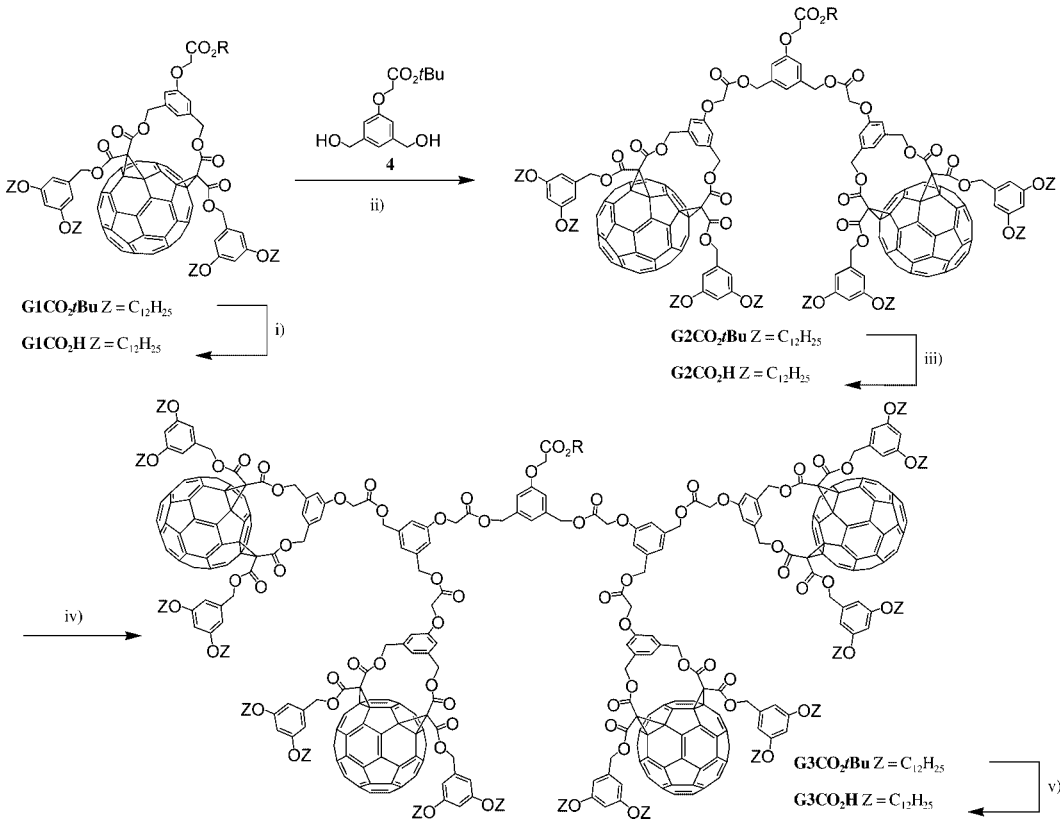


Scheme 1. i) $CF_3CO_2H$, $CH_2Cl_2$, rt (99%); ii) DCC, DMAP, HOBt, $CH_2Cl_2$, 0°C to rt (67%); iii) $CF_3CO_2H$, $CH_2Cl_2$, rt (99%); iv) **4**, DCC, DMAP, HOBt, $CH_2Cl_2$, 0°C to rt (85%); v) $CF_3CO_2H$, $CH_2Cl_2$, rt (96%).

lene)-tethered fullerene *cis-2* bis-adducts.[10] Effectively, in addition to the signals arising from the 3,5-didodecyloxybenzyl units, an AB quartet is observed for the diastereotopic benzylic $CH_2$ group ($H_{A\text{-}B}$) and an $AX_2$ system for the aromatic protons of the 1,3,5-trisubstituted bridging phenyl ring ($H_{3\text{-}4}$). For **G2CO$_2$*t*Bu**, the signals corresponding to the central *tert*-butyl [3,5-bis(methylene)phenoxy]acetate are clearly observed: an $AX_2$ system is revealed for the aromatic protons ($H_{5\text{-}6}$), two singlets for the methylene units $H_F$ and $H_G$ as well as a singlet for the methyl groups of the *tert*-butyl moiety at $\delta$ 1.51 ppm. Finally, it can be noted that the resonance of the methylenic protons $H_E$ is slightly down-field shifted when the corresponding acetate unit is connected to a benzylic moiety (**G2CO$_2$*t*Bu**) rather to a *tert*-butyl subunit (**G1CO$_2$*t*Bu**).

The preparation of the next generation compound was achieved by repeating the same reaction sequence. Treatment of **G2CO$_2$*t*Bu** with $CF_3CO_2H$ in $CH_2Cl_2$ afforded **G2CO$_2$H** in high yield (99%) and subsequent esterification with diol **4** (DCC/DMAP/HOBt) gave **G3CO$_2$*t*Bu** in 85% yield. This compound was characterized by $^1$H and $^{13}$C NMR, MALDI-TOF mass spectrometry and elemental analysis. As shown in Figure 1, the $^1$H NMR spectrum of **G3CO$_2$*t*Bu** clearly reveals the signals corresponding to three [3,5-bis-(methylene)phenoxy]acetate subunits in a 4:2:1 ratio in full agreement with the proposed dendritic structure. Finally, hydrolysis of the *tert*-butyl ester group under acidic conditions afforded the third generation carboxylic acid **G3CO$_2$H**.

The preparation of the central OPV core bearing two alcohol units[11] allowing further attachment of **G1–3CO$_2$H** under DCC-mediated esterification conditions is described in Scheme 2. Treatment of tetraethyleneglycol (TEG) with

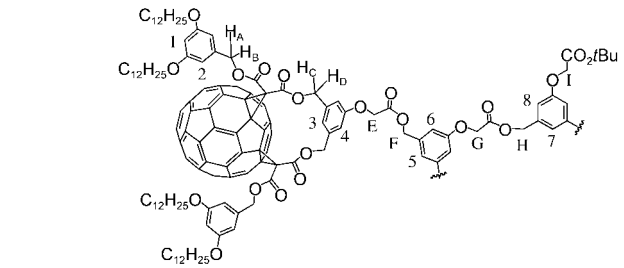

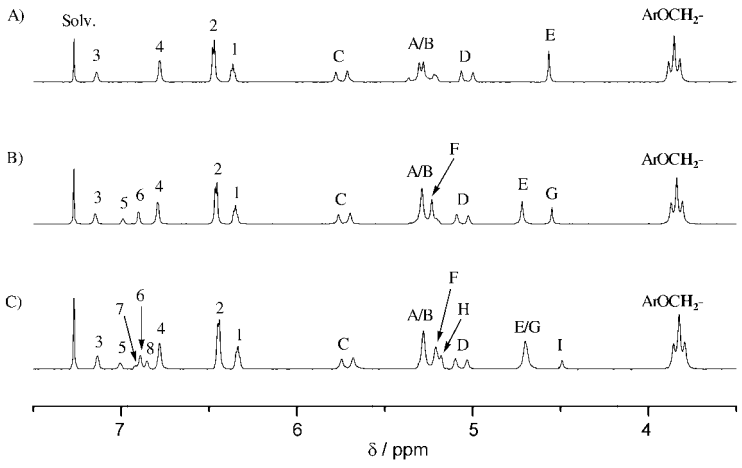


Figure 1. $^1$H NMR spectra ($CDCl_3$, 200 MHz) of **G1CO$_2$*t*Bu** (A); **G2CO$_2$*t*Bu** (B) and **G3CO$_2$*t*Bu** (C).

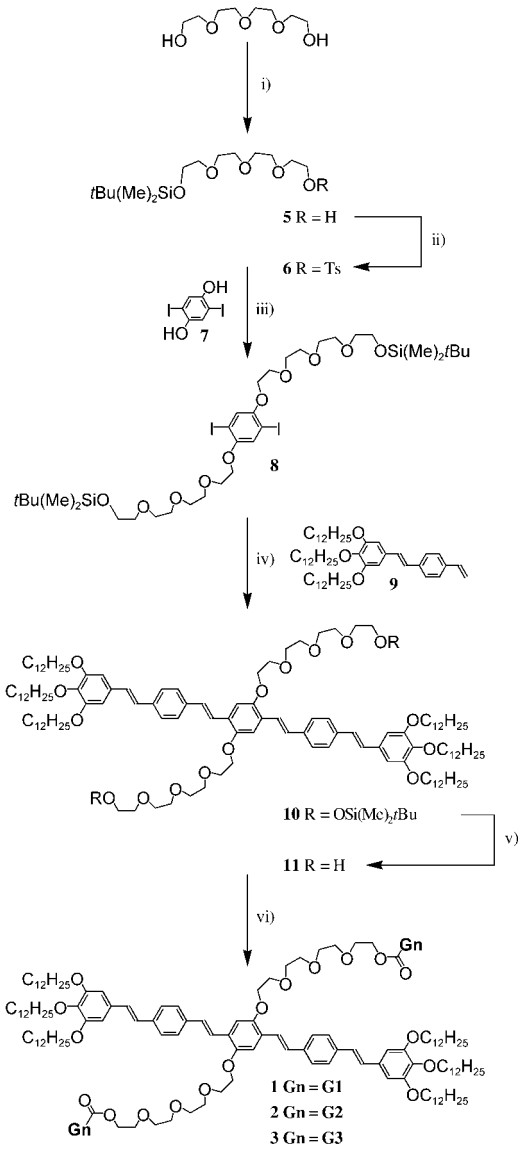

Scheme 2. i) TBDMSCl (1 equiv), imidazole, DMF, 0°C (48%); ii) TsCl, pyridine, DMAP, $CH_2Cl_2$, 0°C (60%); iii) $K_2CO_3$, DMF, 80°C (76%); iv) $Pd(OAc)_2$, TOP, $Et_3N$, xylene, 80°C (61%); v) TBAF, THF, 0°C (90%); vi) **GnCO$_2$H**, DCC, DMAP, HOBt, $CH_2Cl_2$, 0°C to rt (**1**: 87% from **G1CO$_2$H**; **2**: 59% from **G2CO$_2$H**; **3**: 70% from **G3CO$_2$H**).

1 equiv *tert*-butyldimethylsilyl chloride (TBDMSCl) afforded the mono-protected derivative **5** which after reaction with tosyl chloride (TsCl) in the presence of pyridine and DMAP yielded **6**. 2,5-Diiodohydroquinone (**7**) was prepared in two steps from 1,4-dimethoxybenzene as previously described by Weder and Wrighton.[12] Treatment of **7** with tosylate **6** in DMF at 80°C in the presence of $K_2CO_3$ gave the alkylation product **8** in 76% yield. The preparation of the OPV derivative **10** was then based on Heck-type chemistry.[13] Thus, reaction of **8** with styrene **9**[14] in $Et_3N$/xylene in the presence of tri-*o*-tolylphosphine (POT) and a catalytic amount of $Pd(OAc)_2$ afforded **10** in 61% yield (Scheme 2).

  

Subsequent treatment with tetra-*n*-butylammonium fluoride (TBAF) in THF gave diol **11** in 90% yield.

The first generation derivative **1** was obtained in 87% yield by esterification of diol **11** with **G1CO$_2$H** (Scheme 2). Fullerodendrimer **1** was characterized by $^1$H and $^{13}$C NMR, MALDI-TOF mass spectrometry and elemental analysis. The mass spectrum of **1** displays only one peak at *m*/*z* 5978 corresponding to the expected molecular ion peak (calcd *m*/*z* 5977.9). The $^1$H NMR spectrum of fullerodendrimer **1** recorded in $CDCl_3$ is in full agreement with the proposed centrosymmetric structure (Figure 2). Unambiguous assignment was achieved on the basis of 2D-COSY and NOESY spectra recorded at room temperature in $CDCl_3$. The spectrum of **1** shows all the characteristic features of the **G1CO$_2$** moieties already discussed for **G1–3CO$_2$*t*Bu**. The spectrum is also characterized by three sets of signals for the aromatic protons of the central OPV core unit: an AA′XX′ system for $H_{l\text{-}m}$ and two singlets corresponding to $H_i$ and $H_p$. Two AB quartets are observed for the vinylic protons of the OPV backbone ($H_{j\text{-}k}$ and $H_{n\text{-}o}$). Importantly, coupling constants of about 17 Hz confirmed the all-*E* stereochemistry of the π-conjugated system in **1**.

Fullerodendrimers **2** and **3** were prepared by DCC-mediated esterification of diol **11** with **G2CO$_2$H** and **G3CO$_2$H**, respectively. The structure of both **2** and **3** was confirmed by mass spectrometry. The expected molecular ion peak is observed at *m*/*z* 10368 for **2** (calcd *m*/*z* 10367.2) and *m*/*z* 19144 for **3** (calcd *m*/*z* 19145.7). In both cases, characteristic fragments are also observed. In particular, hydrolysis of one or two 3,5-didodecyloxybenzylic ester followed by a decarboxylation is observed, leading to signals at $[M^+-C_{32}H_{55}O_4]$ and $[M^+-2\times(C_{32}H_{55}O_4)]$. However, no signals corresponding to defected dendrimers could be detected, thus showing the monodispersity of both **2** and **3**. In spite of the high molecular weights of dendrimers **2** and **3**, their $^1$H NMR spectra are well resolved (Figure 3). For both compounds, complete assignment was possible on the basis of 2D-COSY and NOESY spectra. The spectrum of **2** reveals all the signals arising from the OPV core unit as well as the typical resonances of the **G2CO$_2$** groups. Similarly, the characteristic signals of the core unit as well as those of the surrounding dendrons are clearly seen in the $^1$H NMR spectrum of **3**.

## Photophysical properties

***Reference compounds***: The electronic absorption spectrum of the bis-methanofullerene **G1CO$_2$*t*Bu** (Figure 4) shows very intense bands in the UV side and much weaker features in the Vis spectral region with the peak corresponding to the lowest allowed singlet transition[15] at 437 nm ($\varepsilon$ = 3100 $M^{-1}cm^{-1}$). The shape of the absorption spectra of **G2CO$_2$*t*Bu** and **G3CO$_2$*t*Bu** are identical to that of **G1CO$_2$*t*Bu** with molar extinction coefficients two and four times larger, respectively (Figure 4). Absorption shapes of the dendronic fullerene reference units **G*n*-3CO$_2$*t*Bu** are substantially unchanged in toluene (PhMe) and benzonitrile (PhCN), relative to $CH_2Cl_2$, over the whole spectral range.

In $CH_2Cl_2$ **G1CO$_2$*t*Bu** exhibits a fluorescence band peaked, after correction for the instrumental response, at the border between the Vis and the IR region ($\lambda_{max}$ = 778 nm, $\Phi$ = 0.0003, $\tau$ = 1.6 ns), inset of Figure 4. Within experimental uncertainty (see Experimental Section), these parameters are unaffected in **G2CO$_2$*t*Bu** and **G3CO$_2$*t*Bu** even by changing to PhMe and PhCN solvents.

An intense triplet–triplet transient absorption spectrum is recorded for **G1–3CO$_2$*t*Bu** in $CH_2Cl_2$, with a maximum at 720 nm. The spectral decay is monoexponential for **G1CO$_2$*t*Bu** and biexponential for **G2CO$_2$*t*Bu** and **G3CO$_2$*t*Bu** (Figure 5).

The intensity of the shorter-lived component (about 100 ns) increases with the laser energy and, at the same excitation energy, is more pronounced for **G3CO$_2$*t*Bu** than for

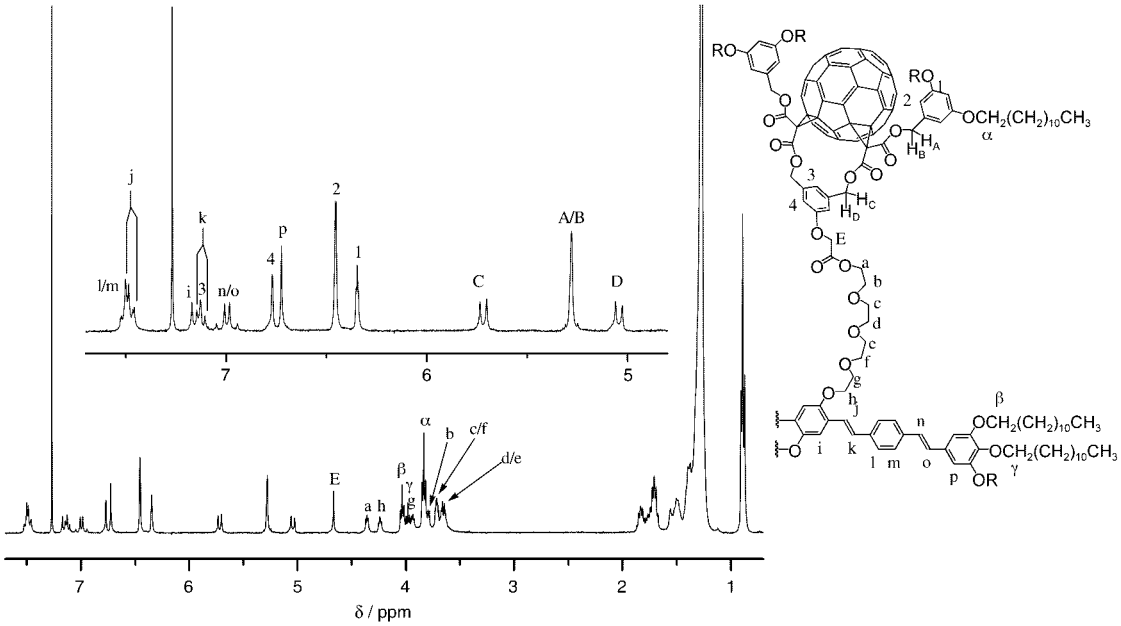


Figure 2. $^1$H NMR spectrum ($CDCl_3$, 400 MHz) of fullerodendrimer **1**.

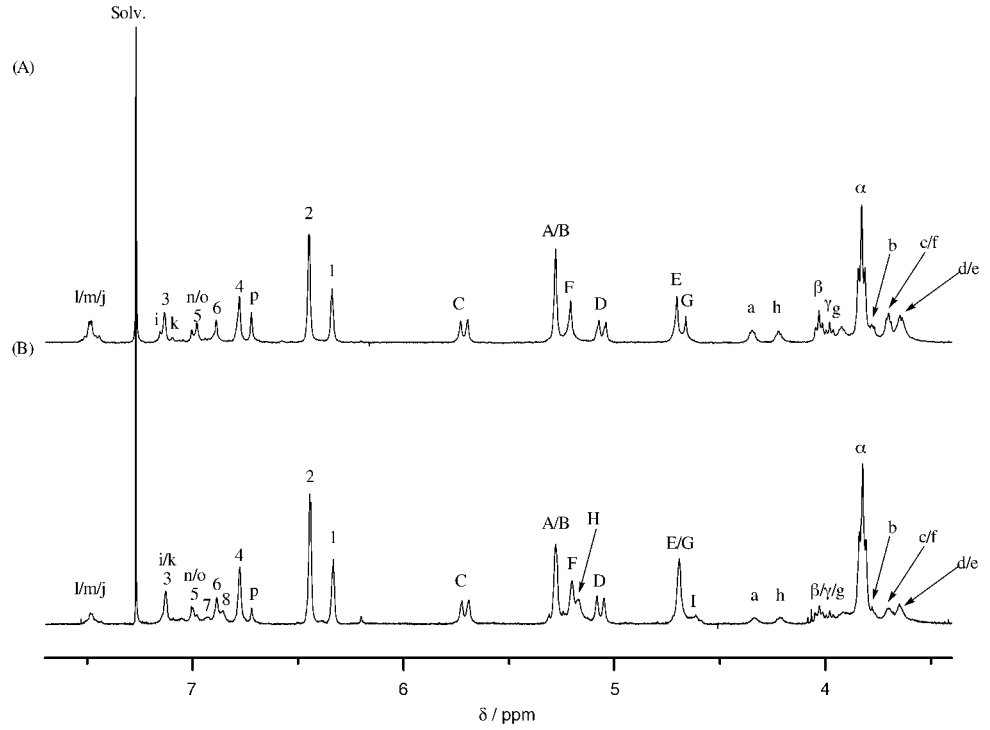


Figure 3. $^1$H NMR spectra ($CDCl_3$, 400 MHz) of **2** (A) and **3** (B).

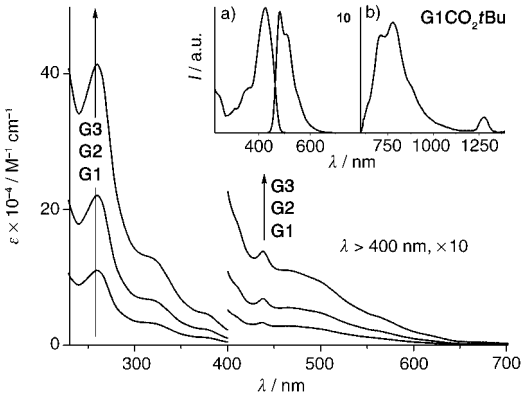


Figure 4. Absorption spectra of **G1CO$_2$*t*Bu** (G1); **G2CO$_2$*t*Bu** (G2) and **G3CO$_2$*t*Bu** (G3) in $CH_2Cl_2$; in the region above 400 nm a multiplying factor of 10 is applied. Inset: a) absorption and fluorescence spectra of **10** ($\lambda_{exc}=425$ nm); b) fluorescence spectrum of **G1CO$_2$*t*Bu** ($\lambda_{exc}=530$ nm) and sensitized singlet oxygen luminescence band ($\lambda_{max}=1270$ nm). Luminescence spectra are corrected for the instrumental response.

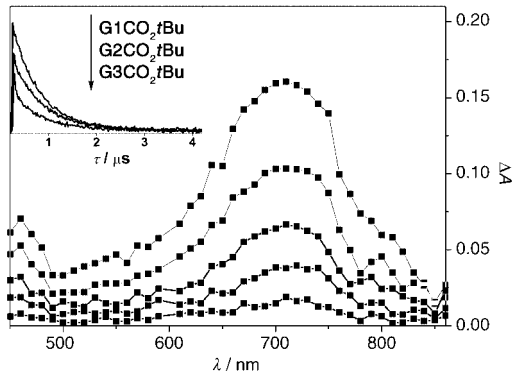


Figure 5. Transient absorption spectrum of **G1CO$_2$*t*Bu** at 298 K in $CH_2Cl_2$ air-purged solution upon laser excitation at 355 nm (2 mJ pulse$^{-1}$). The spectra were recorded at delays of 2, 10, 20, 30, 50 μs following excitation. The inset shows decay time profiles (720 nm) of **G1CO$_2$*t*Bu**, **G2CO$_2$*t*Bu** and **G3CO$_2$*t*Bu** at high energy laser input (20 mJ pulse$^{-1}$, $A=$ 0.50, air equilibrated samples). This evidences the size-dependent short-lived component, in parallel with the decrease of the signal of the "regular" triplet decay, attributed to T–T annihilation processes.

**G2CO$_2$*t*Bu**. These observations suggest the occurrence of intramolecular triplet–triplet annihilation processes[16] in **G2CO$_2$*t*Bu** and **G3CO$_2$*t*Bu** which bear dimeric and tetrameric fullerene arms. The probability of such excited state interactions, which are observable only under intense laser light irradiation, is higher when the number of carbon spheres per dendrimer molecule is larger. The long-lived component of the triplet decays of **G2CO$_2$*t*Bu** and **G3CO$_2$*t*Bu** are coincident and identical to that of **G1CO$_2$*t*Bu** ($\tau=600\pm30$ ns and $18\pm1$ μs in air-equilibrated and air-free solution, respectively). Similar excitation intensity dependent triplet-triplet annihilation processes have been observed earlier in $C_{60}$ fine particles.[17]

The absorption and emission spectra in $CH_2Cl_2$ of the OPV reference derivative **10** are depicted in Figure 4. As is typical for OPV-type molecules, it exhibits intense and short-lived fluorescence ($\lambda_{max}=483$ nm, $\Phi=0.52$, $\tau=1.0$ ns), which can be conveniently used to monitor the occurrence of OPV/$C_{60}$ excited state interactions (see below).[2b,d,3a,5,18,19]

***Dendrimers***: The absorption spectra of **1–3** in $CH_2Cl_2$ solution are shown in Figure 6. Both the features of the fullerene moiety (UV side and above 500 nm) and those of the OPV chromophore (maximum or shoulder around 425 nm)

  

are observable. The spectra of the multicomponent arrays are not well superimposed to the profiles obtained by summing the contribution of each chromophoric moiety. Specifically, the absorption of the OPV core is less than expected and the effect is more and more pronounced by increasing the dendrimer size. As an example, in Figure 6 the spectrum of **3** is compared to the profile calculated for its component subunits (2 **G3CO$_2$*t*Bu + 10**). On the contrary, in the regions where the absorption of the fullerene moiety is prevalent or exclusive experimental and calculated spectra are in excellent agreement. This trend may suggest a modification of the solvation environment for the central OPV core by increasing the dendrimers size. A similar effect has been found for fullerodendrimers having the carbon sphere as central unit.[10d,20,21]

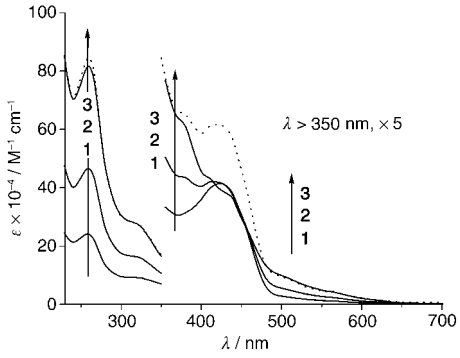


Figure 6. Absorption spectra in $CH_2Cl_2$ of **1–3** (——). The dotted spectrum represents the sum of (2 × **G3CO$_2$*t*Bu + 10**); in the region above 350 nm a multiplying factor of 10 is applied.

Relative to the reference OPV, the fluorescence band of the central chromophore is strongly quenched in dendrimers **1–3** ($CH_2Cl_2$, $\lambda_{exc}$ = 425 nm, $c \leq 5\times10^{-6}$ M). Excitation spectra taken at 800 nm (fullerene fluorescence) exhibit the intense fullerene band at 260 nm but also the contribution of the OPV absorption at 425 nm indicating that the OPV quenching is due to singlet–singlet ($^1$OPV*→$^1$C$_{60}$*) energy transfer, in line with previous reports on OPV–C$_{60}$ hybrids.[2b,d,3a,5,18,19] Model calculations to evaluate the rate of energy transfer[2b] are hampered by the fact that **1–3** are flexible structures where the distance between the single central unit and the multiple external carbon cages is hardly predictable. One cannot exclude, especially in more polar solvents (see below), that there is close vicinity (through space) between OPV and C$_{60}$ subunits. Quenching factors of the OPV fluorescence in $CH_2Cl_2$ ($\Phi_{ref}/\Phi$) are 125, 150, and 210 for **1**,**2**, and **3**, respectively. In the latter case the quenching factor is the highest despite the fact that in an ideal extended structure the OPV–C$_{60}$ distance is the longest. This supports the view of folded compact structures for the largest dendrimer with short intercomponent distances between the energy transfer couples.

For **2**, the dendrimer exhibiting intermediate quenching factor, we estimate a rate constant for the energy transfer process of $1.5\times10^{11}$ s$^{-1}$ [Eq. (1)]. This corresponds to a quenched lifetime of 6.7 ps, well below our instrumental time resolution.[2b,18]

$$k_{EnT} = \frac{\left(\frac{\Phi_{ref}}{\Phi} - 1\right)}{\tau_{ref}} \quad (1)$$

In Equation (1) $\Phi$ and $\Phi_{ref}$ are, respectively, the OPV fluorescence quantum yield of the dendrimers and of the reference compound, whereas $\tau_{ref}$ is the singlet lifetime of the latter.

Photoinduced electron transfer in OPV–C$_{60}$ arrays has been obtained in solution from the lowest fullerene singlet excited state (~1.7 eV), directly or indirectly populated following light absorption.[2d,3a] On the contrary, population of upper lying OPV singlet levels (> 2.8 eV) does not result in electron transfer since competitive ultrafast energy-transfer prevails.[2b,3a,5] Thus electron transfer in OPV–C$_{60}$ systems can be conveniently signaled by the quenching of C$_{60}$ fluorescence and can be observed or not depending on the solvent polarity (Figure 7).[2d,3a]

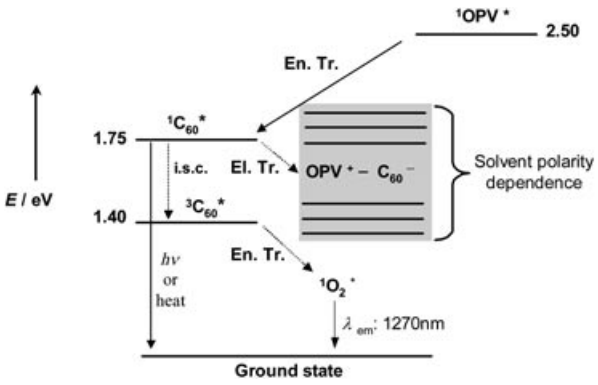


Figure 7. Typical energy-level diagram of rigid OPV–C$_{60}$ arrays describing intrinsic and intercomponent processes following light excitation of the OPV subunit. Electron transfer only occurs from the fullerene singlet state and may be switched on/off by solvent polarity, which allows energy tuning of the charge separated state below/above the fullerene singlet.

In Figures 8–10 (top) are reported the fluorescence spectra of **1–3**, compared with those of the corresponding reference fullerene systems **G1–3CO$_2$*t*Bu** under the same conditions in solvent of increasing polarity. We used toluene (PhMe), dichloromethane ($CH_2Cl_2$), and benzonitrile (PhCN), which exhibit static relative permittivity $\varepsilon$ of 2.4, 8.9, and 25.2 respectively.[22]

In PhMe solution (Figure 8) the fullerene-type fluorescence is unquenched relative to the model compounds for the whole **1–3** family. This signals the absence of OPV→C$_{60}$ electron transfer upon population of the fullerene singlet state in apolar toluene, as observed in OPV–C$_{60}$ arrays investigated earlier.[2d,3a] It is interesting to note that, in any solvent, the quantum yield of singlet oxygen sensitization of the dendrimers is about 15% lower than that of the corresponding reference compounds. In principle this could indicate that, to some extent, electron transfer is promoted by the fullerene triplet level. This process, never reported for

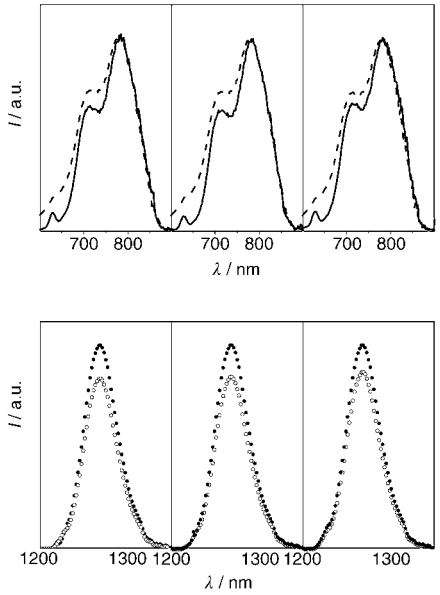


Figure 8. Top, from left to right: Corrected emission spectra of **1–3** (-----) and their reference compounds **G1–3CO$_2$*t*Bu** (——) in $PhCH_3$; $\lambda_{exc}$= 425 nm or $\lambda_{exc}$=530 nm. Bottom, in the same order: Sensitized singlet oxygen emission in $PhCH_3$ of **1–3** (○) and their reference compounds **G1–3CO$_2$*t*Bu** (●) ; $\lambda_{exc}$=500 nm. $A$=0.30 for all compounds.

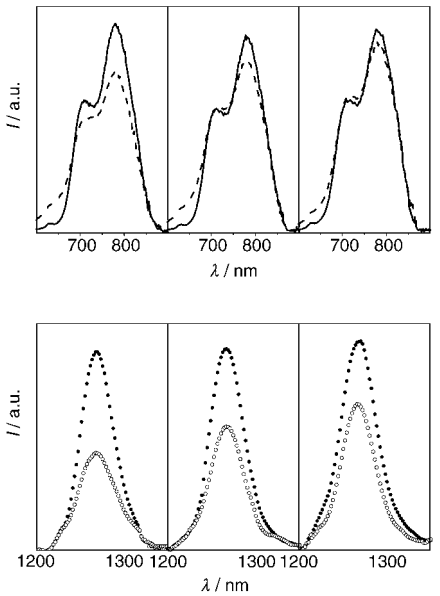


Figure 9. Top, from left to right: Corrected emission spectra of **1–3** (-----) and their reference compounds **G1–3CO$_2$*t*Bu** (——) in $CH_2Cl_2$; $\lambda_{exc}$= 425 nm or $\lambda_{exc}$=530 nm. Bottom, in the same order: Sensitized singlet oxygen emission in $CH_2Cl_2$ of **1–3** (○) and their reference compounds **G1–3CO$_2$*t*Bu** (●); $\lambda_{exc}$=500 nm. $A$=0.30 for all compounds.

rigid OPV–$C_{60}$ systems, might take place in the present flexible arrays where interchromophoric distance is difficult to predict and short distance between the carbon sphere and the central OPV chromophore could be achieved, especially in polar solvents. However this hypothesis is discarded since electron transfer from the fullerene triplet is thermodynamically not allowed (see below) and this is confirmed by the absence of triplet lifetime quenching for **1–3** relative to the fullerene model compounds, whatever the solvent. Thus we attribute the decrease of the singlet oxygen sensitization yield to peculiar intramolecular contacts occurring in the dendrimer structures, which decrease the surface of the fullerene cages available for dioxygen bimolecular interactions.[23]

In $CH_2Cl_2$, from electrochemical potentials,[24] the energy of the OPV$^+$–$C_{60}^-$ charge separated state of **1** is estimated to be 1.68 eV,[25] that is, almost isoenergetic to the fullerene singlet (Figure 7). Similar energetics do not allow electron transfer in rigid OPV–$C_{60}$ arrays, owing to an activation barrier of about 0.2 eV.[2d] Clearly, in the present flexible systems where electron transfer partners can get in tighter vicinity, such barrier is lower and electron transfer can occur, as suggested by the decrease of fullerene fluorescence for **1** (Figure 9, top left). A more marked effect on fullerene fluorescence in polar PhCN supports this interpretation (Figure 10, top left).[6] The lifetime of the fullerene moiety of **1** is 750 ps, compared to 1600 ps of the reference moiety **G1CO$_2$*t*Bu**, corresponding to an electron transfer rate constant of $7.1\times10^8\ s^{-1}$ in benzonitrile.

Interestingly, for larger dendrimers **2** and **3** there is recovery of fluorescence intensity in both in $CH_2Cl_2$ and in PhCN, suggesting a decreased electron transfer efficiency, despite the fact that electron transfer partners and thermodynamics are identical to **1**. Practically no electron transfer from fullerene singlet occurs for **3** in $CH_2Cl_2$ (Figure 9, top right), whereas some of it is still detected in the more polar PhCN (Figure 10, top right). These trends can be rationalized by considering increasingly compact dendrimer structures in more polar solvents.[26] This implies that the actual polarity experienced by the involved electron transfer partners, par-

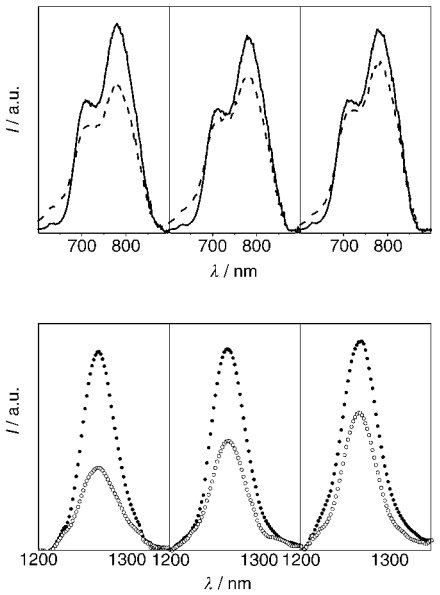


Figure 10. Top, from left to right: Corrected emission spectra of **1–3** (-----) and their reference compounds **G1–3CO$_2$*t*Bu** (——) in PhCN; $\lambda_{exc}$=425 nm or $\lambda_{exc}$=530 nm. Bottom, in the same order: Sensitized singlet oxygen emission in PhCN of **1–3** (○) and their reference compounds **G1–3CO$_2$*t*Bu** (●); $\lambda_{exc}$=500 nm. $A$=0.30 for all compounds.

  

ticularly the central OPV, is no longer that of the bulk solvent. This strongly affects electron transfer thermodynamics which, being reasonably located in the normal region of the Marcus parabola,[2d,3a] becomes less exergonic and thus slower and less competitive towards intrinsic deactivation of the fullerene singlet state. This dendritic effect is in line with the molecular dynamics studies which suggest that the central OPV unit is more and more protected by the dendritic branches when the generation number is increased. Actually, the calculated structure of **3** shows that the two dendrons of third generation are able to fully cover the central OPV core (Figure S1).

The trend of sensitized singlet oxygen luminescence resembles that of fullerene fluorescence, since the detected signal is more intense by increasing the dendrimer size, confirming the above mentioned polarity effects. However, as in the case of PhMe solvent, the amount of fullerene triplet (indirectly monitored via NIR singlet oxygen emission)[2d,23] is comparably lower than that of singlet (probed by fullerene fluorescence). This behavior is in contrast to what was observed in rigid OPV–$C_{60}$ arrays where the relative amount of fullerene fluorescence intensity and sensitized singlet oxygen are identical.[2d] Similarly to what discussed on PhMe solvent (see above) we exclude that any electron transfer from the triplet state occurs, since triplet lifetimes of **1–3** are unchanged relative to the fullerene models **G1–3CO$_2$*t*Bu**. Thus we attribute reduced singlet oxygen sensitization to structural factors which, in polar solvents where the compactness of the dendrimers structure is probably enhanced, are expected to play an even major role.

## Conclusion

A new series of dendrimers with an OPV core and peripheral fullerene subunits have been prepared. Their photophysical properties have been systematically investigated in different solvents and singular polarity effects resulting from the dendritic structure evidenced. Actually, the photophysical properties of the first generation compound are similar to those already reported for related OPV–fullerene systems.[2d,3a] Specifically, photoinduced electron transfer originating from the fullerene singlet excited state has been found dramatically solvent dependent,[2d,3a] because the energy of the charge separated state can be finely tuned around the energy value exhibited by the fullerene singlet excited state (~1.7 eV). In other words, solvent polarity can affect the electron transfer energetics and transform an endoergonic process in a moderately exergonic one, by switching from apolar (e.g. PhMe) to more polar media (e.g. PhCN). In contrast, for the highest generation dendrimer, the strong solvent effects on the OPV–$C_{60}$ charge separation processes are severely limited. For a given solvent, the extent of electron transfer is reduced with dendrimers size because progressive isolation of the central OPV electron donor by the surrounding dendrons tends to disfavor solvent induced stabilization of the transient ionic species. The dendritic architecture is therefore not only able to isolate the central core unit but it can also influence dramatically its properties.

## Experimental Section

**General**: Reagents and solvents were purchased as reagent grade and used without further purification. THF was distilled over sodium/benzophenone. Compounds **G1CO$_2$*t*Bu**,[8] **G1CO$_2$H**,[8] **4**,[8] **7**,[12] and **9**[14] were prepared according to previously reported procedures. The preparation of **G2–3CO$_2$H** and **11** is described in the Supporting Information. All reactions were performed in standard glassware under an inert Ar atmosphere. Evaporation and concentration were done at water aspirator pressure and drying in vacuo at $10^{-2}$ Torr. Column chromatography: silica gel 60 (230–400 mesh, 0.040–0.063 mm) was purchased from E. Merck. Thin-layer chromatography (TLC) was performed on glass sheets coated with silica gel 60 $F_{254}$ purchased from E. Merck, visualization by UV light. NMR spectra were recorded on a Bruker AC 200 (200 MHz) or a Bruker AM 400 (400 MHz) with solvent peaks as reference. Mass measurement were carried out on a Bruker Biflex matrix-assisted laser desorption time-of-flight mass spectrometer (MALDI-TOF) equipped with Scout High Resolution Optics, an *X*–*Y* multi-sample probe and a gridless reflector. Ionization is accomplished with the 337 nm beam from a nitrogen laser with a repetition rate of 3 Hz. All data were acquired at a maximum accelerating potential of 20 kV in the linear positive ion mode. The output signal from the detector was digitized at a sampling rate of 1 GHz. A saturated solution of 1,8,9-trihydroxyanthracene (dithranol ALDRICH EC: 214-538-0) in $CH_2Cl_2$ was used as a matrix. Typically, a 1:1 mixture of the sample solution in $CH_2Cl_2$ was mixed with the matrix solution and 0.5 μL of the resulting mixture was deposited on the probe tip. Calibration was performed in the external mode with insulin (5734.6 Da) and ACTH (2465.2 Da). Elemental analyses were performed by the analytical service at the Institut Charles Sadron, Strasbourg.

**Compound 1**: DCC (58 mg, 0.28 mmol) was added to a stirred solution of **G1CO$_2$H** (300 mg, 0.145 mmol), **11** (140 mg, 0.07 mmol), DMAP (9 mg, 0.07 mmol) and HOBt (10 mg, 0.07 mmol) in $CH_2Cl_2$ (10 mL) at 0°C. After 1 h, the mixture was allowed to slowly warm to room temperature (within 1 h), then stirred for 24 h, filtered and evaporated. Column chromatography (silica gel, $CH_2Cl_2$/0.2% MeOH) yielded **1** (369 mg, 87%) as a dark orange glassy product. IR ($CH_2Cl_2$): $\tilde{\nu}$ = 1745 (C=O); $^1$H NMR ($CDCl_3$, 400 MHz): $\delta$ = 0.89 (t, $J$ = 6 Hz, 42H), 1.26 (m, 252H), 1.70 (m, 16H), 1.83 (m, 12H), 3.64 (m, 8H), 3.66 (m. 8H), 3.79 (m, 4H), 3.83 (t, $J$ = 6 Hz, 16H), 3.93 (m, 4H), 3.98 (t, $J$ = 6 Hz, 4H), 4.03 (t, $J$ = 6 Hz, 8H), 4.24 (t, $J$ = 5 Hz, 4H), 4,36 (t, $J$ = 5 Hz, 4H), 4.67 (s, 4H), 5.04 (d, $J$ = 13 Hz, 4H), 5.28 (s, 8H), 5.72 (d, $J$ = 13 Hz, 4H), 6.34 (t, $J$ = 2 Hz, 4H), 6.45 (d, $J$ = 2 Hz, 8H), 6.72 (s, 4H), 6.77 (s, 4H), 6.99 (AB, $J$ = 17 Hz, 4H), 7.10 (d, $J$ = 17 Hz, 2H), 7.12 (s, 2H), 7.17 (s, 2H), 7.46 (d, $J$ = 17 Hz, 2H), 7.49 (AA′XX′, $J$ = 7 Hz, 8H); $^{13}$C NMR ($CDCl_3$, 50 MHz): $\delta$ = 14.1, 22.6, 25.7, 26.0, 26.1, 29.2, 29.3, 29.4, 29.6, 29.7, 29.8, 30.4, 31.9, 49.0, 63.1, 64.3, 65.3, 66.8, 67.1, 68.0, 68.7, 68.8, 69.1, 69.9, 70.5, 70.6, 70.7, 70.9, 73.5, 101.6, 105.2, 107.1, 111.2, 112.5, 116.0, 122.9, 126.6, 126.9, 127.3, 128.7, 132.5, 134.3, 135.7, 136.0, 136.5, 136.6, 137.0, 137.7, 138.3, 139.9, 141.0, 141.1, 142.2, 142.6, 143.15, 143.5, 143.7, 143.9, 144.1, 144.2, 144.5, 144.8, 144.9, 145.1, 145.3, 145.5, 145.6, 145.7, 146.0, 147.3, 147.4, 148.6, 151.1, 153.3, 157.8, 160.3, 162.4, 162.5, 168.4; MALDI-TOF-MS: calcd for $C_{402}H_{442}O_{44}$: 5977.9; found: 5978; elemental analysis calcd (%) for $C_{402}H_{442}O_{44}$: C 80.77, H 7.45; found: C 80.54, H 7.54.

**Compound 2**: DCC (36 mg, 0.17 mmol) was added to a stirred solution of **G2CO$_2$H** (401 mg, 0.095 mmol), **11** (85 mg, 0.043 mmol), DMAP (9 mg, 0.07 mmol) and HOBt (10 mg, 0.07 mmol) in $CH_2Cl_2$ (10 mL) at 0°C. After 1 h, the mixture was allowed to slowly warm to room temperature (within 1 h), then stirred for 48 h, filtered and evaporated. Column chromatography (silica gel, $CH_2Cl_2$/0.2% MeOH) yielded **2** (264 mg, 59%) as a dark orange glassy product. IR ($CH_2Cl_2$): $\tilde{\nu}$ = 1745 (C=O); $^1$H NMR ($CDCl_3$, 400 MHz): $\delta$ = 0.89 (t, $J$ = 6 Hz, 66H), 1.26 (m, 396H), 1.70 (m, 32H), 1.83 (m, 12H), 3.64 (m, 8H), 3.70 (m, 8H), 3.78 (m, 4H), 3.83 (t, $J$ = 6 Hz, 32H), 3.92 (m, 4H), 3.98 (t, $J$ = 6 Hz, 4H), 4.03 (t, $J$ = 6 Hz, 8H), 4.22 (m, 4H), 4.35 (m, 4H), 4.66 (s, 4H), 4.70 (s, 8H), 5.06 (d, $J$ = 13 Hz, 8H), 5.21 (s, 8H), 5.28 (s, 16H), 5.71 (d, $J$ = 13 Hz, 8H), 6.34 (t, $J$ = 2 Hz, 8H), 6.45 (d, $J$ = 2 Hz, 16H), 6.72 (s, 4H), 6.78 (s, 8H), 6.88 (s, 4H), 6.98 (s, 2H), 7.00 (d, $J$ = 17 Hz, 4H), 7.10 (d, $J$ = 17 Hz, 2H), 7.13 (s, 4H), 7.45 (d, $J$ = 17 Hz, 2H), 7.48 (AA′XX′, $J$ = 7 Hz, 8H); $^{13}$C NMR ($CDCl_3$, 50 MHz): $\delta$ = 14.0, 22.6, 26.0, 29.2, 29.3, 29.4, 29.6, 30.3, 31.8, 48.96, 63.0, 64.2, 65.1, 65.3, 66.3, 66.7, 67.0, 68.0, 68.6, 68.7, 69.1, 69.8, 70.4, 70.5, 70.6, 70.8, 73.4, 101.5, 105.1, 107.0, 111.1, 112.4, 114.5, 116.0,

121.2, 122.9, 126.6, 126.8, 127.2, 128.7, 132.4, 134.3, 135.6, 135.9, 136.4, 136.6, 136.9, 137.2, 137.7, 138.3, 138.4, 138.8, 139.9, 140.9, 141.0, 142.1, 142.6, 143.0, 143.4, 143.6, 143.8, 144.0, 144.2, 144.5, 144.8, 144.9, 145.0, 145.2, 145.4, 145.6, 145.9, 147.2, 147.3, 148.5, 151.0, 153.2, 157.7, 158.1, 160.3, 162.4, 162.5, 168.2, 168.3; MALDI-TOF-MS: calcd for $C_{698}H_{698}O_{80}$: 10367.2; found: 10368 [$M^+$]; elemental analysis calcd (%) for $C_{698}H_{698}O_{80}$: C 80.87, H 6.79; found C 80.84, H 6.77.

**Compound 3**: DCC (22 mg, 0.11 mmol) was added to a stirred solution of **G3CO$_2$H** (515 mg, 0.060 mmol), **11** (53 mg, 0.027 mmol), DMAP (9 mg, 0.07 mmol) and HOBt (10 mg, 0.07 mmol) in $CH_2Cl_2$ (10 mL) at 0 °C. After 1 h, the mixture was allowed to slowly warm to room temperature (within 1 h), then stirred for 48 h, filtered and evaporated. Column chromatography (silica gel, $CH_2Cl_2$/0.2 % MeOH) yielded **3** (364 mg, 70 %) as a dark orange glassy product. IR ($CH_2Cl_2$): $\tilde{\nu}$ = 1745 (C=O); $^1$H NMR ($CDCl_3$, 400 MHz): $\delta$ = 0.89 (t, $J$ = 6 Hz, 114 H), 1.27 (m, 684 H), 1.70 (m, 64 H), 1.82 (m, 12 H), 3.65 (m, 8 H), 3.70 (m, 8 H), 3.77 (m, 4 H), 3.82 (t, $J$ = 6 Hz, 64 H), 3.91 (m, 4 H), 3.98 (t, $J$ = 6 Hz, 4 H), 4.02 (t, $J$ = 6 Hz, 8 H), 4.21 (m, 4 H), 4.33 (m, 4 H), 4.61 (s, 4 H), 4.69 (s, 24 H), 5,06 (d, $J$ = 13 Hz, 16 H), 5.17 (s, 8 H), 5.20 (s, 16 H), 5.28 (s, 32 H), 5.71 (d, $J$ = 13 Hz, 16 H), 6.33 (t, $J$ = 2 Hz, 16 H), 6.44 (d, $J$ = 2 Hz, 32 H), 6,72 (s, 4 H), 6.78 (s, 16 H), 6.86 (s, 4 H), 6.88 (s, 8 H), 6.92 (s, 2 H), 6.97 (s, 4 H), 7.00 (AB, $J$ = 17 Hz, 4 H), 7.12 (m, 10 H), 7.47 (m, 10 H); $^{13}$C NMR ($CDCl_3$, 50 MHz): $\delta$ = 14.1, 22.6, 26.0, 29.2, 29.3, 29.4, 29.6, 31.9, 48.9, 65.3, 66.3, 66.7, 67.0, 68.0, 68.7, 69.1, 70.5, 70.8, 73.5, 101.5, 105.1, 107.1, 112.4, 114.5, 115.9, 121.3, 126.6, 126.8, 127.2, 128.7, 132.4, 134.3, 135.6, 135.9, 136.4, 136.6, 137.2, 137.3, 137.7, 138.4, 139.9, 140.9, 141.0, 142.1, 142.6, 143.1, 143.5, 143.6, 143.8, 144.0, 144.2, 144.5, 144.8, 144.9, 145.0, 145.2, 145.5, 145.6,; 145.9, 147.2, 147.3, 148.5, 151.0, 153.2, 157.7, 158.0, 160.3, 162.5, 162.6, 168.2; MALDI-TOF-MS: calcd for $C_{1290}H_{1210}O_{152}$: 19145.7; found: 19144 [$M^+$]; elemental analysis calcd for $C_{1290}H_{1210}O_{152}$: C 80.93, H 6.37; found: C 80.70, H 6.62.

**Photophysical measurements**: The photophysical investigations were carried out in toluene, dichloromethane, and benzonitrile solutions (Carlo Erba or Aldrich spectrofluorimetric grade). The path of fluorimetric cuvettes was 1 cm. Absorption spectra were recorded with a Perkin-Elmer $\lambda$ 45 spectrophotometer. Uncorrected emission spectra were obtained with a Spex Fluorlog II spectrofluorimeter (continuous 150 W Xe lamp), equipped with Hamamatsu R-928 photomultiplier tube. The corrected spectra were obtained *via* a calibration curve determined with a procedure described earlier.[27] The steady-state NIR luminescence spectra were obtained with an Edinburgh FLS920 spectrometer equipped with Hamamatsu R5509-72 supercooled photomultiplier tube (193 K) and a TM300 emission monochromator with NIR grating blazed at 1000 nm. An Edinburgh Xe900 450 W Xenon arc amp was used as light source; the emission calibration curve was supplied by the manufacturer. Emission lifetimes were determined with (i) an IBH single photon counting spectrometer equipped with a thyratron gated nitrogen lamp (2–40 kHz, $\lambda_{exc}$ = 337 nm, 500 ps time resolution) and a Hamamatsu 3237-01 photomultiplayer tube (185–850 nm) or ii) an Edinburgh FLS920 spectrometer equipped with laser diode heads (1 MHz, $\lambda_{exc}$ = 407 or 635 nm, 100 ps time resolution) and a peltier-cooled Hamamatsu R928 photomultiplayer tube (185–850 nm). Transient absorption spectra in the nanosecond-microsecond time domain were obtained with a flash-photolysis system described in detail earlier.[28] Excitation was performed with the second or third harmonic (532/355 nm) of a Nd:YAG laser (J. K. Lasers Ltd.) with 20 ns pulse duration and 1–2 mJ of energy per pulse (up to 20 mJ for energy-dependent triple-triplet annihilation processes). Triplet lifetimes were obtained by averaging at least five different decays recorded around the maximum of the absorption peak (720 nm). When necessary, oxygen was removed by at least four freeze-thaw-pump cycles by means of a diffusive vacuum pump at $10^{-6}$ Torr. Experimental uncertainties are estimated to be 7 % for lifetime determinations, ±20 % for emission quantum yields, and 2 % for absorption and emission peaks.

## Acknowledgements

This work was supported by the CNR, the CNRS, the French Ministry of Research (ACI Jeunes Chercheurs to J.-F.N.) and EU (RTN Contract "FAMOUS", HPRN-CT-2002-00171). G.A. thanks Italian MIUR (contract FIRB RBNE019H9K, Molecular Manipulation for Nanometric Machines) and M.G.N. the CONACyT for their reasearch fellowships. We further thank L. Oswald for technical help, Dr. C. Bourgogne for his help for the molecular modeling, Prof. M. Gross and Dr. J.-P. Gisselbrecht for the CV measurements, J.-M. Strub for the MALDI-TOF mass spectra and M. Schmitt for high field NMR measurements.

[1] a) N. Armaroli, in *Fullerenes: from synthesis to optoelectronic properties* (Eds.: D. M. Guldi, N. Martin), Kluwer, Dordrecht, **2002**, pp. 137–162; b) P. J. Brecher, D. Schuster, in *Fullerenes: from synthesis to optoelectronic properties* (Eds.: D. M. Guldi, N. Martin), Kluwer, Dordrecht, **2002**, pp. 163–212; c) D. M. Guldi, M. Prato, *Acc. Chem. Res.* **2000**, *33*, 695–703; d) N. Martín, L. Sánchez, B. Illescas, I. Pérez, *Chem. Rev.* **1998**, *98*, 2527–2547; e) H. Imahori, Y. Sakata, *Eur. J. Org. Chem.* **1999**, 2445–2457; f) D. Gust, T. A. Moore, A. L. Moore, *Acc. Chem. Res.* **2001**, *34*, 40–48.

[2] a) J.-F. Nierengarten, J.-F. Eckert, J.-F. Nicoud, L. Ouali, V. Krasnikov, G. Hadziioannou, *Chem. Commun.* **1999**, 617–618; b) J.-F. Eckert, J.-F. Nicoud, J.-F. Nierengarten, S.-G. Liu, L. Echegoyen, F. Barigelletti, N. Armaroli, L. Ouali, V. Krasnikov, G. Hadziioannou, *J. Am. Chem. Soc.* **2000**, *122*, 7467–7479; c) T. Gu, D. Tsamouras, C. Melzer, V. Krasnikov, J.-P. Gisselbrecht, M. Gross, G. Hadziioannou, J.-F. Nierengarten, *ChemPhysChem* **2002**, *3*, 124–127; d) N. Armaroli, G. Accorsi, J.-P. Gisselbrecht, M. Gross, V. Krasnikov, D. Tsamouras, G. Hadziioannou, M. J. Gomez-Escalonilla, F. Langa, J.-F. Eckert, J.-F. Nierengarten, *J. Mater. Chem.* **2002**, *12*, 2077–2087; e) J.-F. Nierengarten, T. Gu, T. Aernouts, W. Geens, J. Poortmans, G. Hadziioannou, D. Tsamouras, *Appl. Phys. A* **2004**, *79*, 47–49.

[3] a) E. Peeters, P. A. van Hal, J. Knol, C. J. Brabec, N. S. Sariciftci, J. C. Hummelen, R. A. J. Janssen, *J. Phys. Chem. B* **2000**, *104*, 10174–10190; b) D. M. Guldi, C. Luo, A. Swartz, R. Gomez, J. L. Segura, N. Martin, C. Brabec, S. Sariciftci, *J. Org. Chem.* **2002**, *67*, 1141–1152; c) M. Maggini, G. Possamai, E. Menna, G. Scorrano, N. Camaioni, G. Ridolfi, G. Casalbore-Miceli, L. Franco, M. Ruzzi, C. Corvaja, *Chem. Commun.* **2002**, 2028–2029; d) N. Negishi, K. Yamada, K. Takimiya, Y. Aso, T. Otsubo, Y. Harima, *Chem. Lett.* **2003**, 404.

[4] For a review on fullerene–(π-conjugated oligomer) dyads as active photovoltaic materials, see: J.-F. Nierengarten, *Sol. Energy Mater. Sol. Cells* **2004**, *83*, 187–199.

[5] N. Armaroli, F. Barigelletti, P. Ceroni, J.-F. Eckert, J.-F. Nicoud, J.-F. Nierengarten, *Chem. Commun.* **2000**, 599–600.

[6] a) T. Gu, J.-F. Nierengarten, *Tetrahedron Lett.* **2001**, *42*, 3175–3178; b) T. Yamashiro, Y. Aso, T. Otsubo, H. Tang, Y. Harima, K. Yamashita, *Chem. Lett.* **1999**, 443–444; c) Y. Obara, K. Takimiya, Y. Aso, T. Otsubo, *Tetrahedron Lett.* ***2001***, *42*, 6877–6880; d) S.-G. Liu, L. Shu, J. Rivera, H. Liu, J.-M. Raimundo, J. Roncali, A. Gorgues, L. Echegoyen, *J. Org. Chem.* **1999**, *64*, 4884–4886; e) J. L. Segura, R. Gomez, N. Martin, D. M. Guldi, *Chem. Commun.* **2000**, 701–702; f) F. Effenberger, G. Grube, *Synthesis* **1998**, 1372–1379; g) for a review on fullerene–(π-conjugated oligomer) dyad, see: J. L. Segura, N. Martin, D. M. Guldi, *Chem. Soc. Rev.* **2004**, in press.

[7] a) G. Accorsi, N. Armaroli, J.-F. Eckert, J.-F. Nierengarten, *Tetrahedron Lett.* **2002**, *43*, 65–68; b) D. M. Guldi, A. Swartz, C. Luo, R. Gomez, J. L. Segura, N. Martin, *J. Am. Chem. Soc.* **2002**, *124*, 10875–10886; c) F. Langa, M. J. Gomez-Escalonilla, E. Diez-Barra, J. C. Garcia-Martinez, A. de la Hoz, J. Rodriguez-Lopez, A. Gonzalez-Cortes, V. Lopez-Arza, *Tetrahedron Lett.* **2001**, *42*, 3435–3438; d) A. G. Avent, P. R. Birkett, F. Paolucci, S. Roffia, R. Taylor, N. K. Wachter, *J. Chem. Soc. Perkin Trans. 2* **2000**, 1409–1412.

[8] D. Felder, M. Gutiérrez Nava, M. P. Carreon, J.-F. Eckert, M. Luccisano, C. Schall, P. Masson, J.-L. Gallani, B. Heinrich, D. Guillon, J.-F. Nierengarten, *Helv. Chim. Acta* **2002**, *85*, 288–319.

[9] a) J.-F. Nierengarten, *Top. Curr. Chem.* **2003**, *228*, 87–110; b) J.-F. Nierengarten, *Chem. Eur. J.* **2000**, *6*, 3667–3670; c) J.-F. Nierengarten, D. Felder, J.-F. Nicoud, *Tetrahedron Lett.* **1999**, *40*, 269–272; d) J.-F. Nierengarten, D. Felder, J.-F. Nicoud, *Tetrahedron Lett.* **1999**, *40*, 273–276; e) J.-F. Nierengarten, D. Felder, J.-F. Nicoud, *Tetrahedron Lett.* **2000**, *41*, 41–44; f) D. Felder, H. Nierengarten, J.-P. Gis-

  

selbrecht, C. Boudon, E. Leize, J.-F. Nicoud, M. Gross, A. Van Dorsselaer, J.-F. Nierengarten, *New J. Chem.* **2000**, *24*, 687–695.

[10] a) Y. Rio, G. Enderlin, C. Bourgogne, J.-F. Nierengarten, J.-P. Gisselbrecht, M. Gross, G. Accorsi, N. Armaroli, *Inorg. Chem.* **2003**, *42*, 8783–8793; b) S. Zhang, Y. Rio, F. Cardinali, C. Bourgogne, J.-L. Gallani, J.-F. Nierengarten, *J. Org. Chem.* **2003**, *68*, 9787–9797; c) F. Cardinali, J.-F. Nierengarten, *Tetrahedron Lett.* **2003**, *44*, 2673–2676; d) Y. Rio, G. Accorsi, H. Nierengarten, C. Bourgogne, J.-M. Strub, A. Van Dorsselaer, N. Armaroli, J.-F. Nierengarten, *Tetrahedron* **2003**, *59*, 3833–3844; e) M. Gutiérrez-Nava, S. Setayesh, A. Rameau, P. Masson, J.-F. Nierengarten, *New J. Chem.* **2002**, *26*, 1584–1589.

[11] OPV derivative **11** has been used for the synthesis of linear polymers alternating OPV moieties and $C_{60}$ subunits and its preparation has been briefly described in a preliminary communication: M. Gutiérrez-Nava, P. Masson, J.-F. Nierengarten, *Tetrahedron Lett.* **2003**, *44*, 4487–4490.

[12] C. Weder, M. S. Wrighton, *Macromolecules* **1996**, *29*, 5157–5165.

[13] F. H. Heck, *Palladium Reagents in Organic Synthesis*, Academic Press, London, **1985**.

[14] Compound **9** was obtained in six steps from methyl 3,4,5-trihydroxybenzoate as described in: T. Gu, P. Ceroni, G. Marconi, N. Armaroli, J.-F. Nierengarten, *J. Org. Chem.* **2001**, *66*, 6432–6439.

[15] N. Armaroli, C. Boudon, D. Felder, J.-P. Gisselbrecht, M. Gross, G. Marconi, J.-F. Nicoud, J.-F. Nierengarten, V. Vicinelli, *Angew. Chem.* **1999**, *111*, 3895–3899; *Angew. Chem. Int. Ed.* **1999**, *38*, 3730–3733.

[16] K. D. Ausman, R. B. Weisman, *Res. Chem. Intermed.* **1997**, *23*, 431–451.

[17] M. Fujitsuka, H. Kasai, A. Masuhara, S. Okada, H. Oikawa, H. Nakanishi, O. Ito, K. Yase, *J. Photochem. Photobiol. A* **2000**, *133*, 45–50.

[18] P. A. van Hal, R. A. J. Janssen, G. Lanzani, G. Cerullo, M. Zavelani-Rossi, S. De Silvestri, *Phys. Rev. B* **2001**, *64*, 075206.

[19] A. Marcos Ramos, M. T. Rispens, J. K. J. van Duren, J. C. Hummelen, R. A. J. Janssen, *J. Am. Chem. Soc.* **2001**, *123*, 6714–6715.

[20] Y. Murata, M. Ito, K. Komatsu, *J. Mater. Chem.* **2002**, *12*, 2009–2020.

[21] Y. Rio, G. Accorsi, H. Nierengarten, J. L. Rehspringer, B. Honerlage, G. Kopitkovas, A. Chugreev, A. Van Dorsselaer, N. Armaroli, J. F. Nierengarten, *New J. Chem.* **2002**, *26*, 1146–1154.

[22] S. L. Murov, I. Carmichael, G. L. Hug, *Handbook of Photochemistry*, Marcel Dekker, New York, **1993**.

[23] N. Armaroli, G. Accorsi, D. Felder, J. F. Nierengarten, *Chem. Eur. J.* **2002**, *8*, 2314–2323.

[24] V. Balzani, F. Scandola, *Supramolecular Photochemistry*, Ellis Horwood, Chichester (UK), **1991**, pp. 44–45.

[25] The electrochemical properties of **1**, **2** and **3** have been investigated by cyclic voltammetry in $CH_2Cl_2$/0.1 M $Bu_4NBF_4$. For the three compounds, the redox potential of the first reduction (centered on the peripheral fullerene units) is observed at −1.10 V vs $Fc^+$/Fc and the redox potential of the first oxidation (centered on the OPV core unit) at +0.58 V vs $Fc^+$/Fc. M. Gross, J.-P. Gisselbrecht, unpublished results.

[26] J.-F. Nierengarten, N. Armaroli, G. Accorsi, Y. Rio, J.-F. Eckert, *Chem. Eur. J.* **2003**, *9*, 37–41.

[27] N. Armaroli, G. Marconi, L. Echegoyen, J.-P. Bourgeois, F. Diederich, *Chem. Eur. J.* **2000**, *6*, 1629–1645.

[28] L. Flamigni, *J. Phys. Chem.* **1992**, *96*, 3331–3337.

Received: February 17, 2004
Revised: June 23, 2004
Published online: August 20, 2004